

Stress-dilatancy behaviour of frozen sand in direct shear

N. Yasufuku

Kyushu University, Fukuoka, Japan

S.M. Springman, L.U. Arenson & T. Ramholt

Institute for Geotechnical Engineering, Swiss Federal Institute of Technology, Zurich, Switzerland

ABSTRACT: This paper aims to clarify the characteristics of the strength and dilatancy behaviour of saturated frozen sand in direct shear. A series of direct shear box tests were performed in a cold room using saturated frozen fine sand samples with a wide range of sand volume fractions. The dependency of the strength and dilatancy behaviour on the temperature, normal stress and strain rate are discussed on the basis of the experimental results. It was found that the shear strength and dilatancy of the sand-ice mixture was strongly dependent on the rate of shear deformation and the volume fraction of sand. The ongoing dilation of most of the tests indicates that the shearing not only affects a thin shear plane, but also influences strongly the adjacent soil due to possible propagation of cracks between the solid particles. Furthermore, the shear strength was quite sensitive to the temperature changes in the ranges near to 0°C.

1 INTRODUCTION

The importance of high mountain permafrost as a natural hazard is increasing, due to indications of increasing rising global temperatures (Cheng & Dramis 1992, Haeberli et al. 1993, 1997, Knutti et al. 2002). The melting of ice in the permafrost matrix will reduce the inter-particle stress and hence shear strength. This may, in the presence of water, quickly lead to slope failure and debris flows (Haefeli 1948, Iverson & Major 1986, Haeberli et al. 1997, Arenson & Springman 2000). In Switzerland, the population in Alpine valleys is quite dense and debris flows can cause much damage and even loss of life (Haeberli et al. 1990, Zimmermann 1990). Hence, the potential for instability of Alpine permafrost has been identified as being an issue of considerable importance in Switzerland (Haeberli et al. 1999).

Although the dangers are known, the knowledge of the thermo-mechanical behaviour of Alpine permafrost is limited. Until now, Alpine permafrost research has focused mainly on issues such as geomorphological aspects, measurements of internal and surface movements and temperatures, general structure of the ground or age of the permafrost (e.g. Haeberli et al. 1998, Vonder Mühll et al. 1998, Käb & Vollmer 2000). Therefore, advanced knowledge of the mechanical properties of thawing permafrost is required for numerical modelling, and to enable predictions of

potential slope instabilities due to temperature changes.

Based on measurements of internal deformation of creeping rock glaciers in the Swiss Alps (e.g. Arenson et al. 2002) a distinct shear zone from some centimetres up to metres thick, where up to 97% of the rock glacier deformation occurs, could be located. Direct shear box tests have been proposed in order to model this shear zone and to determine the mobilised strength on a plane.

In the study presented in this paper, a series of direct shear box tests were performed in a cold room, using laboratory prepared saturated frozen fine sand samples with various sand contents. Temperature dependency between -3 and -7°C, and effects of normal stress and strain rate dependency on the strength-dilatancy behaviour are discussed on the basis of experimental results and microscopic observations of the specimens after shearing.

2 MATERIALS AND TESTING PROCEDURES

2.1 *Testing programme*

Table 1 shows the test conditions of the direct shearing under constant normal stress on frozen Weiacher fine sand. In order to clarify the effects of volume fraction of sand f_s on the direct shear strength of frozen sands, f_s was varied from 0.05 to 0.63 in which f_s is defined as $1/(1+e)$, with e as the voids ratio. Three horizontal deformation rates, i.e.

horizontal deformation velocities, dH/dt were applied: 2.0 mm/min, 0.2 mm/min and 0.02 mm/min. Normal stresses σ_{v0} were selected from a range between 200 kPa and 400 kPa based on the recorded depths of *in situ* shear surfaces. The testing temperatures were -6.5, -4.1 and -3.1°C, respectively.

Table 1. Test conditions.

Temp. T (°C)	Normal stress σ_{v0} (kPa)	dH/dt 2 mm/min		dH/dt 0.2 mm/min				dH/dt 0.02 mm/min			
		f_s		f_s				f_s			
-3.1	200	0.17	0.43	0.05	0.17	0.35	0.43	0.57	0.63	0.17	0.43
	300	x	x							x	x
	400			x		x	x	x		x	x
-4.1	200			x		x					
	300	x	x	x	x	x	x	x		x	x
	400			x		x					
-6.5	200										
	300			x	x	x	x	x	x		
	400										

Figure 1 shows the direct shear box, which was kept in a cold room at the specific test temperature within an accuracy of $\pm 0.5^\circ\text{C}$. A sensor was mounted in the lower half of the box, to measure the temperature of the specimen. Corresponding temperatures in the sample varied by $\pm 0.3^\circ\text{C}$.

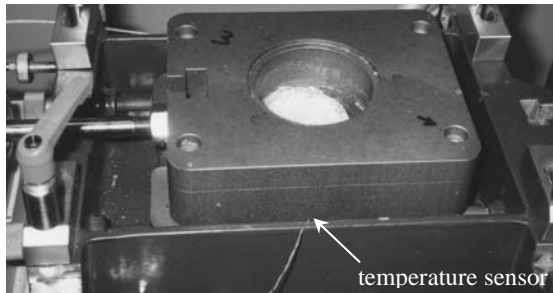


Figure 1. Direct shear box, diameter = 6.5 cm.

2.2 Sample preparation

Weiacher fine silica sand was used as an inclusion material. The grain size distribution curve of this sand is given in Figure 2. The angle of friction ϕ' of dry Weiacher sand is $\sim 32^\circ$ in simple shear.

The artificially made sand-ice specimens were prepared as follows:

- a known amount of sand was mixed uniformly with powdered ice, that had similar grain sizes to the sand, to prepare a sample with a fixed volume fraction of sand.
- the sand-ice mixture was poured into the shear box and lightly compacted in 4 to 8 layers, depending on the volume fraction of sand.
- the sand-ice specimen was saturated carefully by pouring de-aired water at zero centigrade from the top within the cooling room in order to fill the air

voids without disturbing the packing of the sand-ice mixture.

d) afterwards, the specimen was kept in a freezing box for about 24 hr at a temperature of $-18 \pm 2^\circ\text{C}$ (during the freezing process, the sand particles remained in a dispersed position).

e) the frozen specimen was placed in the direct shear apparatus and left for at least 3 hours until the temperature of the sample became stable. Before shearing, all samples were left for one night after applying the normal stress.

Samples with high sand concentrations ($f_s > 0.55$) were prepared by placing pre-cooled dry sand straight into the direct shear box, pouring pre-cooled water carefully into the sand, and freezing the mixture using a method similar to d) and e).

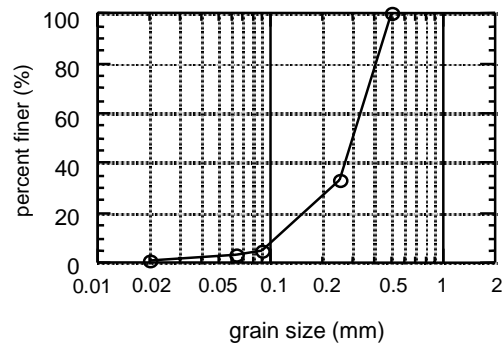


Figure 2. Grain size distribution of Weiacher sand.

The specimens had a diameter of 6.5 cm and a height of about 2.0 cm. Schematic images of sand-ice specimens with low and high sand volume fractions are given in Figure 3.

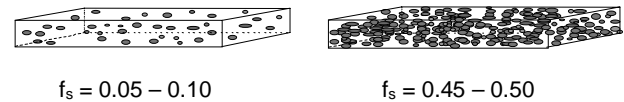


Figure 3. Schematic images of sand-ice specimens.

3 TEST RESULTS AND DISCUSSION

Table 2 summarises test conditions and some key results. Temperatures, volume fraction of sand, applied normal stress and shear deformation rate are shown, together with sample response, including the peak mobilised shear stress, the corresponding horizontal displacement and the mean angle of the dilatancy rate $\nu = \tan^{-1}(dV/dH)$, where V is the vertical and H the horizontal displacement.

Table 2. Summary of test conditions and results.

Test No.	Temp. in specimen (°C)	f_s (-)	σ_{v0} (kPa)	dH/dt (mm/min)	1 st peak shear stress (kPa)	dH at 1 st peak (mm)	peak shear stress (kPa)	mean v (°)
24	-4.1	0.62	100	0.2	1206	3.79	1316	21.8
25	-4.1	0.57	300	0.2	1211	3.79	1357	16.7
27	-4.1	0.43	300	0.2	1160	11.00	1160	14.0
28	-4.1	0.35	300	0.2	920	11.00	920	14.0
30	-4.1	0.05	300	0.2	960	1.32	960	11.3
31	-4.1	0.17	300	0.2	830	1.33	850	12.4
32	-4.1	0.18	300	0.02	515	2.11	515	4.6
33	-4.1	0.17	300	2.0	1209	1.81	1209	18.3
34	-4.1	0.48	300	0.02	725	9.80	725	8.5
35	-4.1	0.43	300	2.0	1442	7.20	1442	18.8
36	-4.1	0.39	200	0.2	959	2.74	1006	14.0
37	-4.1	0.42	400	0.2	960	0.90	1178	11.3
38	-4.1	0.15	200	0.2	856	2.20	856	8.5
39	-4.1	0.18	400	0.2	700	0.74	760	11.3
40	-3.1	0.42	300	0.02	597	10.10	597	4.0
41	-3.1	0.42	300	0.2	965	11.00	965	13.0
42	-3.1	0.39	300	2.0	1409	2.36	1460	6.8
43	-3.1	0.16	300	0.2	818	2.77	786	4.6
44	-3.1	0.16	300	0.02	370	1.00	431	9.1
45	-3.1	0.16	300	2.0	952	1.81	952	14.0
46	-6.5	0.36	300	0.2	1164	8.23	1164	15.6
47	-6.5	0.14	300	0.2	850	8.50	850	5.4
48	-6.5	0.50	300	0.2	1588	9.93	1588	15.6
49	-6.5	0.59	300	0.2	2008	9.23	2008	18.3
50	-6.5	0.31	300	0.2	1046	10.71	1046	10.2
51	-6.5	0.05	300	0.2	987	1.89	987	8.5

3.1 Shear deformation rate dependency

The influence of the horizontal strain rate dH/dt , which was varied from 0.02 to 2 mm/min, on the mobilised shear stress τ and the vertical displacement dV of the ice-soil mixture is shown in Figures 4a and 4b for a relatively low volume fraction of sand ($f_s \approx 0.17$) at a temperature of -4.1°C (Tests 31, 32, 33). Similar results were obtained for a relatively high volume fraction ($f_s \approx 0.43 - 0.48$; Tests 27, 34, 35). The stress-deformation curve and the dilatancy behaviour for the same stress and temperature conditions were found to be strongly dependent on dH/dt . The volume fraction of sand appears to influence the peak mobilised shear stress in a similar manner to the data shown in Figure 4a, but the additional 25 – 30% of sand leads to an increase of maximum shear strength of 200 – 300 kPa under the prevailing normal stress field (Fig. 5). The maximum shear stress increases exponentially with increasing dH/dt for the data shown. The slope of this increase, however, seems not to be influenced by f_s at $T = -4.1^\circ\text{C}$ and $\sigma_{v0} = 300$ kPa. For the same temperature, the dilatancy tends to increase with the increasing dH/dt ($v = 4.6^\circ, 12.4^\circ, 18.3^\circ$).

A close inspection of the shear zone with a microscope (magnification $\times 8$) did not indicate significant expansion of the voids, which may be expected for an unfrozen dilatant material (Fig. 6). In addition, there was no evidence of any other form of damage along the shear zone. If a regelation effect does act around the particles on

the shear plane, there is sufficient free energy available to refreeze liquid water once local shearing is complete. In essence, there is a looser packing in the shear zone due to small dilative movements of the grains combined with self-healing.

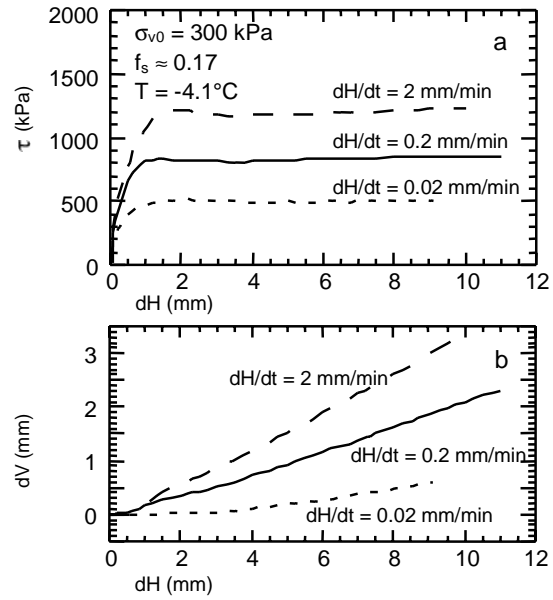


Figure 4. Dependency of deformation rate on strength and dilatancy behaviour due to shear.

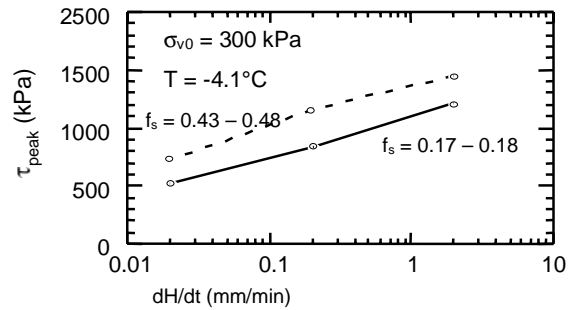


Figure 5. Strength properties of frozen sand related to deformation rate.

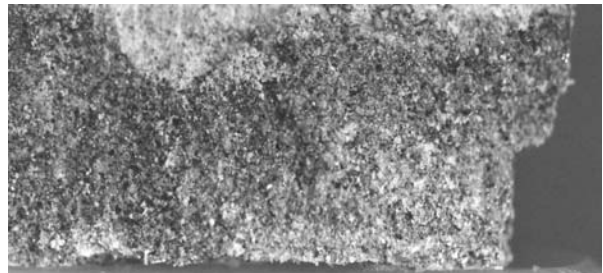


Figure 6. Typical cross section of specimen after shearing (Test 46: $f_s = 0.36$).

3.2 Normal stress dependency

Tests at different values of σ_{v0} showed that there is no significant influence of σ_{v0} on the shear response (Fig. 7a, Tests 31, 38, 39). However, rapid heave was measured at the beginning of the

shearing for the lowest σ_{v0} (Fig. 7b) and this levelled off to a constant value of about 1.5 mm, whereas the behaviour under higher normal stresses is very similar at -4.1°C and $dH/dt = 0.2 \text{ mm/min}$. The tests shown in Figure 7 (Tests 31, 38, 39) are plotted again in Figure 8 with an equivalent series at $f_s = 0.41 \pm 0.02$ (Tests 27, 36, 37) as peak shear strength against normal stress. A slight increase of the shear strength can be determined for $f_s \approx 0.41$, whereas no influence or even a decrease was recorded for $f_s \approx 0.17$. However, the relatively high peak for test No. 38 ($f_s = 0.15$) may be attributed to external work done against the vertical stress as the sample dilates.

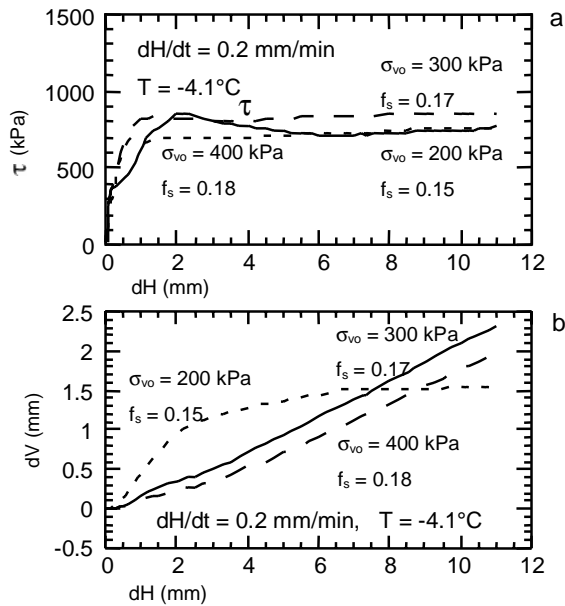


Figure 7. Dependency of (a) shear stress-displacement and (b) dilatancy behaviour on the normal stresses.

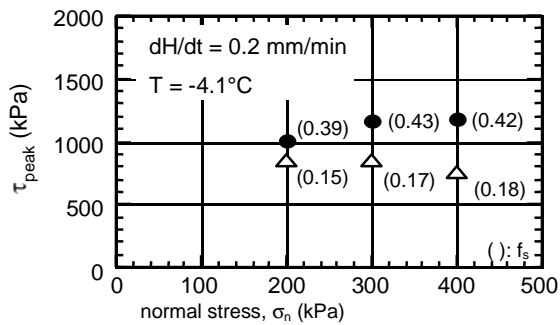


Figure 8. Peak shear strength dependency related to the normal stresses. Closed circles: $f_s \approx 0.41$, open triangles: $f_s \approx 0.17$.

3.3 Volume fraction dependency

Six tests with different volume fractions of sand (Tables 1 & 2: Tests 46-51) were sheared under a normal stress of 300 kPa with a deformation rate of 0.2 mm/min at a temperature of about -6.5°C . The soil particles strongly influenced the response to shearing for $f_s > 0.3$ (Fig. 9a). The yield and the peak shear strength is very similar for low f_s and is

reached within about 2 mm deformation. However, an upper yield region (e.g. Andersen et al. 1995) develops for higher values of f_s , and a strain hardening effect can be observed for the rest of the test.

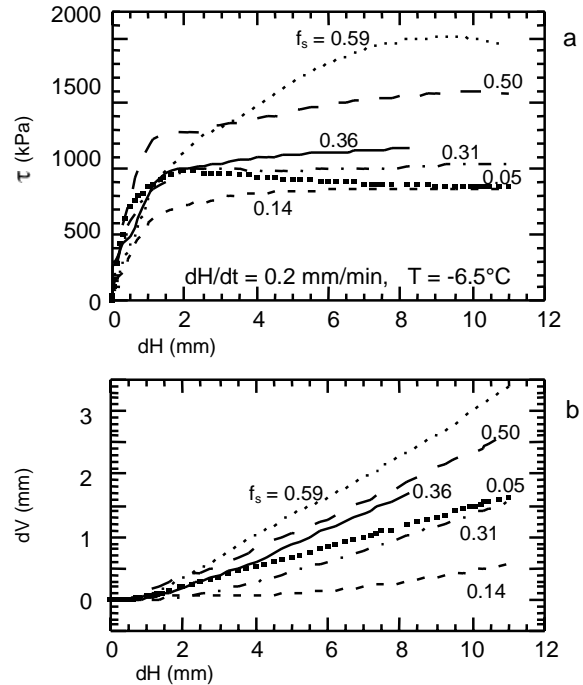


Figure 9. Effect of the volume fraction of sand f_s on (a) the shear stress-deformation and (b) the dilation-deformation relationships.

The dilatancy also changes for different values of f_s . Except for test No. 51 ($f_s = 0.05$), an increase in dilation, and hence v , was recorded with increasing f_s ($v = 8.5^\circ, 5.4^\circ, 10.2^\circ, 15.6^\circ, 15.6^\circ, 18.3^\circ$). It is thought that the greater strength of ice seeded with relatively few solid particles is due to the cracks generated at yield passing from particle to particle, but requiring additional energy to initiate a new crack. However, for such low values of $f_s = 0.05$, the brittle behaviour indicated in Figure 9a is confirmed by the degree of dilation observed in Figure 9b.

Equivalent behaviour was also measured for the tests at -4.1°C (Tests 25, 27, 28, 30, 31) with $v = 11.3^\circ, 12.4^\circ, 14.0^\circ, 14.0^\circ, 16.7^\circ$ respectively. The ongoing dilation shown in Figure 9b is most probably an effect of the crack propagation. In contrast to unfrozen soils, where a shear zone of 5 to 10 grain diameters might be typical, the shear zone within these frozen samples develops to be much larger and therefore more vertical displacement occurs. Stress concentrations that occur around the solid particles result in cracks between the grain bond with the ice matrix that propagate from particle to particle similar to Griffith's (1921) model of fracture for solid materials. The zone affected by these cracks depends on the volume fraction of sand, resulting

in various, but pronounced, dilatancy responses, which seem to question the concept of constant volume for critical state strength (Schofield & Wroth 1968) for frozen soil. Even though a constant value of shear strength was reached for $dH > 10\text{mm}$ the sample height increases, indicating ongoing crack propagation throughout the sample. However, the authors assume that for larger strains, even under the conditions presented, the stress concentration dissipates, stopping further fracturing and a constant value of dV would be attained. This is also a geometrical effect caused by the limitation of the shear box.

During initial phases of shearing (Fig. 10a), the shear zone extends primarily from particle to particle over a depth of approximately 1 – 2 mm. However, as the value of dH increases, the shear zone increases in thickness due to mobilisation of the ice granules and particles acting and dilating together (Fig. 10b). This effect can be described as a “rubblisation” (e.g. Take & Bolton 2002).

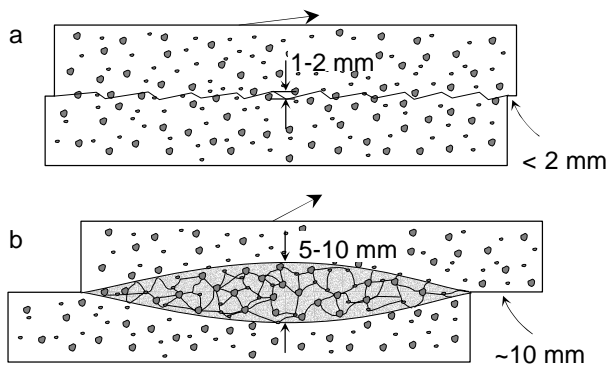


Figure 10. Development of shear zone.

Even though the amount of unfrozen water might be less than 0.05 Vol.-% (Williams 1967, Stähli & Stadler 1997), it may have an additional influence on the behaviour of the sample. The small amount of sand particles in test No. 51 results in very little unfrozen water and therefore supports the concept of brittle behaviour, in contrast to the other tests that showed a ductile tendency. This would also explain why the shear response of this test is higher than the response of test No.47 ($f_s = 0.14$) and why there is a difference in the dilatancy.

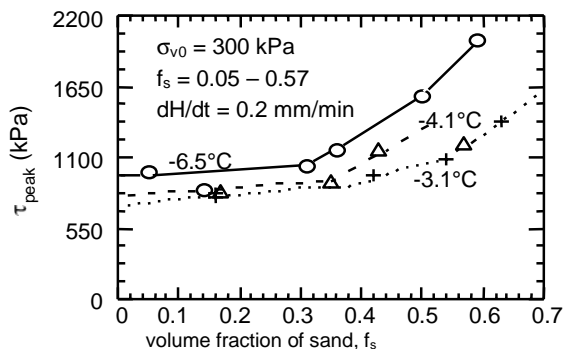


Figure 11. Effect of f_s on peak strength of sand-ice mixture with reference to the temperature of the specimen.

Similar results could be observed for tests at the two other temperatures, -3.1°C and -4.1°C , respectively. Figure 11 shows the effect of f_s on peak strength of the sand-ice mixture with reference to temperature T . There is only a slight increase in the peak strength with decreasing temperature for low f_s . A much steeper increase can be observed for $f_s > 0.3$ and an even steeper increase for $f_s > \sim 0.5$, and this is more pronounced for lower temperatures. Different mechanisms seem to be relevant for the various volume fractions of sand. Several other authors have described this effect. Ting et al. (1983) showed similar results for frozen Ottawa sand at a temperature of -7.6°C under uniaxial compression, suggesting that only the strength of the ice is responsible for the shear strength at low values of f_s . Structural hindrance can be taken into account for volume fractions larger than 0.4, since the solid particles start to come into contact with each other. Crack propagation through the ice-particle mixtures, however, also changes with increasing volume fraction of sand and influences the shear response within the failure plane. Despite the temperature dependency of the ice strength itself, unfrozen water also influences the shear response at warmer temperatures and therefore much lower values for peak strength were measured. Due to the increase of unfrozen water with increasing f_s , a more gentle increase of the shear response with increasing volume fraction of sand occurs.

4 CONCLUSIONS

A series of direct shear box tests were performed on sand-ice mixtures to investigate the effect of volume fraction of sands, normal stresses, strain rate and temperatures between -3.1 and -6.5°C on the dilatancy and strength of such mixtures. The main conclusions can be summarised as follows:

- the vertical deformation due to shearing in a direct shear box was mainly dilative and was strongly dependent on the rate of shear deformation, on the volume fraction of sand as well as on the temperature.
- the shear zone expanded with shear deformation due to crack propagation and “rubblisation” resulting in a pronounced dilatancy that did not level off even at horizontal deformations of more than 10 mm.
- the shear strength of the sand-ice mixture was also dependent on the rate of shear deformation and volume fraction of sand.
- the observed trends were more evident with decreasing temperature: higher peak shear strength was mobilised and proportionally more so at higher f_s .

Mechanisms that are responsible for the shear and the dilatancy behaviour change with different f_s and temperatures. Only the ice controls the response for low f_s . Despite brittle behaviour with a peak shear value at small strain for samples with very low f_s (< 0.1), mainly ductile behaviour with strain hardening and continuous vertical heave was observed for samples with $f_s > 0.1$. Crack propagation might be the main influence that controls the shear and deformation response as a function of the volume fraction of sand, since the solid particles within the ice-soil-matrix control the length and direction of the cracks. In addition, structural hindrance results in higher shear responses and more pronounced dilatancy. Unfrozen water that might also be present under these test conditions has an additional effect that supports a ductile response. An upper yield region develops for small strains and higher f_s . Critical values of f_s , which initiate a change of mechanism, is temperature sensitive, but lies between 0.3 and 0.5. Normal stress seems not to influence the mechanisms significantly.

The presented tests, however, demonstrate the sensitivity of frozen soil response to various effects, such as temperature, deformation rate and volume fraction of sand. Even though direct shear tests have proved to be very suitable for the testing of frozen ice-sand mixtures, further investigations on the change of mechanisms as a function of temperature and grain size distributions are recommended for the future.

ACKNOWLEDGEMENT

The authors wish to acknowledge with gratitude the assistance of IGT/ETHZ personnel with the experiments, particularly D. Bystricky, E. Bleiker and M. Schäfer and Professor F. Bucher for fruitful discussions. The first author also thanks Prof. H. Ochiai and Dr. K. Omine of Kyushu University for supporting him during the sabbatical in Switzerland.

REFERENCES

Andersen, G.R., Swan, C.W., Ladd, C.C. & Germain, J.T. 1995. Small-strain behavior of frozen sand in triaxial compression. *Canadian Geotechnical Journal* 32: 428-451.

Arenson, L. & Springman, S.M. 2000. Slope stability and related problems of Alpine permafrost. *Proc. Int. Workshop Permafrost Engng., Longyearbyen*: 185-196.

Arenson, L.U., Hoelzle, M. & Springman, S.M. 2002. Borehole deformation measurements and internal structure of some rock glaciers in Switzerland. *Permafrost and Periglacial Processes* 13: 117-135.

Cheng, G. & Dramis, F. 1992. Distribution of mountain permafrost and climate. *Permafrost and Periglacial Processes* 3: 83-91.

Griffith, A.A. 1921. The phenomena of rupture and flow in solids. *Philos. Trans. Roy. Soc. London, Ser. A* 221: 163-198.

Haeberli, W., Rickenmann, D. & Zimmermann, M. 1990. Debris flows 1987 in Switzerland: general concept and geophysical soundings. *Hydrology in Mountain Regions. II-Artificial Reservoirs; Water and Slopes, IAHS Publication*: 303-310.

Haeberli, W., Cheng, G., Gorbunov, A.P. & Harris, S.A. 1993. Mountain permafrost and climate change. *Permafrost and Periglacial Processes* 4: 165-174.

Haeberli, W., Wegmann, M. & Vonder Mühll, D. 1997. Slope stability problems related to glacier shrinkage and permafrost degradation in the Alps. *Eclogae Geologicae Helveticae* 90: 407-414.

Haeberli, W., Hoelzle, M., Kääh, A., Keller, F., Vonder Mühll, D. & Wagner, S. 1998. Ten years after drilling through the permafrost of the active rock glacier Murtèl, eastern Swiss Alps: Answered questions and new perspectives. *Proc. 7th Int. Conf. on Permafrost, Yellowknife*: 403-410.

Haeberli, W., Kääh, A., Hoelzle, M., Bösch, H., Funk, M., Vonder Mühll, D. & Keller, F. 1999. *Eisschwund und Naturkatastrophen im Hochgebirge*. Zürich: vdf, Hochschulverlag an der ETH.

Haefeli, R. 1948. The stability of slopes acted upon by parallel seepage. *2nd Int. Conf. On Soil Mech. and Fdn Engng* 1: 57-62.

Iverson, R.M. & Major, J.J. 1986. Groundwater seepage vectors and potential for hillslope failure and debris flow mobilization. *Wat. Resources Res.* 22: 1543-1548.

Kääh, A. & Vollmer, M. 2000. Surface geometry, thickness changes and flow fields on creeping mountain permafrost: Automatic extraction by digital image analysis. *Permafrost and Periglacial Processes* 11: 315-326.

Knutti, R., Stocker, T.F., Joos, F. & Plattner, G.K. 2002. Constraints on radiative forcing and future climate change from observations and climate model ensembles. *Nature* 416: 719-723.

Schofield A.N. & Wroth, C.P. 1968. *Critical State Soil Mechanics*. New York: McGraw-Hill.

Stähli, M. & Stadler D. 1997. Measurement of water and solute dynamics in freezing soil columns with time domain reflectometry. *Journal of Hydrology* 195: 352-369.

Take, W.A. & Bolton, M.D. 2002. The use of centrifuge modelling to investigate progressive failure of overconsolidated clay embankments. In S.M. Springman (ed.), *Constitutive and Centrifuge Modelling: Two Extremes*: 191-197. Lisse, Balkema.

Ting, J., Martin, T & Ladd, C. 1983. Mechanisms of strength for frozen sand. *Journal of Geotechnical Engineering* 109: 1286-1302.

Vonder Mühll, D., Stucki, T. & Haeberli W. 1998. Borehole temperatures in Alpine permafrost: a ten year series. *Proc. 7th Int. Conf. on Permafrost, Yellowknife*: 1089-1095.

Williams, P.J. 1967. Unfrozen water content of frozen soils and soil moisture suction. *Publication of the Norwegian Geotechnical Institute* 72: 11-26.

Zimmermann, M. 1990. Debris flows 1987 in Switzerland: geomorphological and meteorological aspects. *Hydrology in Mountain Regions. II-Artificial Reservoirs; Water and Slopes, IAHS Publication*: 387-393.